

Oblique collisional effects of dust acoustic waves in unmagnetized dusty plasma

M S Alam, M R Talukder

Citation: Chin. Phys. B . 2020, 29(6): 065202 . **doi:** 10.1088/1674-1056/ab829b
Journal homepage: http://cpb.iphy.ac.cn; http://iopscience.iop.org/cpb

What follows is a list of articles you may be interested in

Directional motion of dust particles at different gear structuresin a plasma

Chao-Xing Dai(戴超星), Chao Song(宋超), Zhi-Xiang Zhou(周志向), Wen-Tao Sun(孙文涛), Zhi-Qiang Guo(郭志强), Fu-Cheng Liu(刘富成), Ya-Feng He(贺亚峰)

Chin. Phys. B . 2020, 29(2): 025203 . **doi:** 10.1088/1674-1056/ab6109

Crystalline order and disorder in dusty plasmas investigated by nonequilibrium molecular dynamics simulations

Aamir Shahzad, Maogang He, Sheeba Ghani, Muhammad Kashif, Tariq Munir, Fang Yang

Chin. Phys. B . 2019, 28(5): 055201 . **doi:** 10.1088/1674-1056/28/5/055201

On the dielectric response function and dispersion relation in strongly coupled magnetized dusty plasmas

M Shahmansouri, N Khodabakhshi

Chin. Phys. B . 2018, 27(10): 105206 . **doi:** 10.1088/1674-1056/27/10/105206

Small amplitude double layers in an electronegative dusty plasma with *q*-distributed electrons

Zhong-Zheng Li(李中正), Juan-Fang Han(韩娟芳), Dong-Ning Gao(郜东宁), Wen-Shan Duan(段文山)

Chin. Phys. B . 2018, 27(10): 105204 . **doi:** 10.1088/1674-1056/27/10/105204

Relativistic degenerate effects of electrons and positrons on modulational instability of quantum ion acoustic waves in dense plasmas with two polarity ions

Liu Tie-Lu, Wang Yun-Liang, Lu Yan-Zhen

Chin. Phys. B . 2015, 24(2): 025202 . **doi:** 10.1088/1674-1056/24/2/025202

Oblique collisional effects of dust acoustic waves in unmagnetized dusty plasma

M S Alam[1,†] and M R Talukder[2]

[1] Department of Mathematics, Chittagong University of Engineering and Technology, Chittagong-4349, Bangladesh

[2] Plasma Science and Technology Laboratory, Department of Electrical and Electronic Engineering, University of Rajshahi, Rajshahi-6205, Bangladesh

(Received 7 September 2019; revised manuscript received 9 December 2019; accepted manuscript online 25 March 2020)

Effects of oblique collisions of the dust acoustic (DA) waves in dusty plasma are studied by considering unmagnetized fully ionized plasma. The plasma consists of inertial warm negatively charged massive dusts, positively charged dusts, superthermal kappa distributed electrons, and isothermal ions. The extended Poincaré–Lighthill–Kuo (ePLK) method is employed for the drivation of two-sided Korteweg–de Vries (KdV) equations (KdVEs). The KdV soliton solutions are derived by using the hyperbolic secant method. The effects of superthermality index of electrons, temperature ratio of isothermal ion to electron, and the density ratio of isothermal ions to negatively charged massive dusts on nonlinear coefficients are investigated. The effects of oblique collision on amplitude, phase shift, and potential profile of right traveling solitons of DA waves are also studied. The study reveals that the new nonlinear wave structures are produced in the colliding region due to head-on collision of the two counter propagating DA waves. The nonlinearity is found to decrease with the increasing density ratio of ion to negative dust in the critical region. The phase shifts decrease (increase) with increasing the temperature ratio of ion to electron (κ_e). The hump (compressive, $\kappa_e < \kappa_{ec}$) and dipshaped (rarefactive, $\kappa_e > \kappa_{ec}$) solitons are produced depending on the angle (θ) of oblique collision between the two waves.

Keywords: ion acoustic wave, dusty plasma, kappa distribution, ePLK method, hyperbolic secant method

PACS: 52.27.Ny, 52.35.Fp, 52.35.Mw, 52.30.Cv **DOI:** 10.1088/1674-1056/ab829b

1. Introduction

The charged dusts in plasma exist in space[1–5] (*e.g.* lower and upper mesosphere, cometary tails, planetary rings, planetary magnetospheres, inter-planetary spaces, interstellar media, *etc.*), laboratory experiment (*e.g.* Q-machine, plasma materials processing reactors[1]), *etc*. The wave dynamics, concerning the dust acoustic (DA) waves, dust ion acoustic (DIA) waves, dust acoustic rogue (DAR) waves, *etc.*, facilitate the understanding of the electrostatic density perturbations and potential structures,[6–8] *e.g.*, soliton, shock, rogue profile, vortices, *etc*., as observed in dusty plasma systems. The DA waves are produced[9] due to imbalance between the driving (provided by the inertia of the dust mass) and restoring forces (provided by the thermal pressure of ions and electrons). The linear and nonlinear structures of DA waves in unmagnetized weakly coupled dusty plasmas were investigated theoretically.[10–15]

Mamun *et al.*[16] have investigated the properties of DA solitary and shock waves with strongly coupled electrons and ions by taking into account the Boltzmann (vortex-like) distribution. The positive and negative charged dusts are also observed in space,[4,17–19] such as in upper mesosphere, cometary tails, Jupiter's magneto-sphere, *etc*. The dust grains can be charged positively through three mechanisms:[20] photoemission due to ultraviolet photon flux, thermionic emission induced by radiative heating, and secondary electron emission from the surface of the dust grains. The existence of non-Maxwellian particles is observed from the satellite missions in astrophysical and space plasmas,[21–24] such as in the mercury, uranus, earth, and magnetosphere of Saturn. In these plasmas, the electrons' distribution follows the power-law instead of Maxwellian distribution. On the other hand, the presence of nonthermal particles at high altitudes, *e.g.*, solar wind and space plasmas, is found from the spacecraft observation.[25–29] Besides, the superthermal plasmas are observed in various experimental[30] plasmas, such as laser–matter interactions and plasma turbulence, and their properties are studied by considering the kappa distribution function.[31–33] Kappa distribution was first reported by Vasyliunas[31] to model the space plasmas and latter it was applied to different plasmas by several researchers.

Recently, several authors[34–37] have investigated DIA waves with kappa distributed electrons. Alinejad[37] has shown that the rarefactive DIA solitary waves and double layers may be produced, depending on the population of superthermal electrons. Ghosh *et al.*[38] have investigated the nonlinear properties of DIA solitary waves with small amplitude in dusty plasma comprised of electrons, ions, and dust grains, and found that the wave amplitude exponentially decreases with time due to the collisions of dust ions. Alinejad and Mamun[39] have studied the properties of obliquely propagating electrostatic waves in magnetized plasmas consisting of electrons, ions, and positrons, and noted that the basic features

†Corresponding author. E-mail: alam21nov_2016@yahoo.com

© 2020 Chinese Physical Society and IOP Publishing Ltd

of solitary waves are modified significantly due to oblique collision, densities of superthermal electrons and positrons, and temperature ratio of electron to positron. The productions of solitons and their interactions among themselves are one of the most important nonlinear phenomena in dusty plasmas. Consequently, this has received special attention from plasma researches.

Ghorui *et al.*[40] have studied the characteristics of head-on collisions of counter propagating DIA solitary waves in magnetized quantum dusty plasmas by taking into account positively and negatively charged dust grains and found that the quantum diffraction parameter, ion cyclotron frequency, and density ratio of electron to ion play a significant role in modifying the phase shifts. The head-on collisions between the DA solitary waves have studied by Su and Mirie,[41] Jeffery and Kawahawa,[42] and Huang and Velarde[43] through employing extended Poincaré–Lighthill–Kuo (ePLK) method and found that the characteristic collective motion and collisional properties are affected by the dust charge variation. Xue[44] has also studied the effects of temperature ratio, density ratio of ion to electron, and dust charge variation on phase shifts due to collision of DA solitary waves and noted that the phase shifts are significantly modified by the dust charge variation. Li *et al.*[45] have investigated the interaction among Korteweg–de Vries (KdV) solitons in two-dimensional (2D) dusty plasmas. Besides, Han *et al.*[46] have studied the production of DA solitary waves and their interactions in weakly relativistic 2D thermal plasmas and determined the phase shifts and trajectories for an arbitrary angle of interactions. Chopra[47] has investigated the evolution of DAWs and characterized them in dusty plasmas. On the other hand, Boruah *et al.*[48] have studied the oblique collisional effects in strongly coupled dusty plasma and noted that dust acoustic solitons are formed at a certain collision angle. Das[49] has studied the propagation characteristics of the dust ion acoustic solitary waves in dusty plasma with Boltzmann electrons and found the streaming of dust for both compressive and rarefactive KdV solitons. Zahed *et al.*[50] have found in their study that the amplitude and width of the pseudo-potential have increased with increasing ion. Ferdousi *et al.*[51] have theoretically investigated the characteristic properties of obliquely propagating IASWs in the presence of ambient magnetic field in nonthermal plasma. They have observed that the characteristics of the solitary waves are significantly affected by the nonextensive electrons and positrons as well as external magnetic field. The collisional effects on instabilities of dust acoustic and dust ion acoustic waves were investigated[52] and it was also observed that the dispersion of the dust acoustic and dust ion acoustic waves are reduced due to the superthermal charge particles.

Owing to their importance and significance the oblique interaction phenomena and phase shifts in dusty plasmas are investigated. The plasma, considered here in this work, consists of inertial positively and negatively charged massive dusts, superthermal kappa distributed electrons and isothermal ions. The rest of this paper is organized as follows. In Section 2, the fluid model equations along with the assumptions are presented. In Section 3 the evolution equations and their analytical solutions for determine the phase shifts are derived. The results and discussion are displayed in Section 4. Finally, the results of this work are summarized in Section 5.

2. Assumptions and governing fluid equations

Here, we consider the plasma that consists of inertial warm negatively charged massive dust with mass $m_{1\mathrm{d}}$ and charge $q_1 = -Z_{1\mathrm{d}}e$, positively charged dust with mass $m_{2\mathrm{d}}$ and charge $q_2 = +Z_{2\mathrm{d}}e$, superthermal kappa distributed electrons with mass m_{e} and charge $-e$, and isothermal positive ions with mass m_{i} and charge $+e$, where $Z_{1\mathrm{d}}$ ($Z_{2\mathrm{d}}$) is the charge number of negative (positive) dust. The charge neutrality condition can be defined as $Z_{1\mathrm{d}}n_{1\mathrm{d}0} + n_{\mathrm{e}0} = Z_{2\mathrm{d}}n_{2\mathrm{d}0} + n_{\mathrm{i}0}$, where $n_{1\mathrm{d}0}$, $n_{\mathrm{e}0}$, $n_{2\mathrm{d}0}$, and $n_{\mathrm{i}0}$ are the equilibrium number density of warm negatively charged massive dust, kappa distributed electrons, positively charged dust, and isothermal ions, respectively. The normalized fluid equations of DA waves are considered as[53]

$$\frac{\partial n_{1\mathrm{d}}}{\partial t} + \frac{\partial\left(n_{1\mathrm{d}}u_{1\mathrm{d}}\right)}{\partial x} + \frac{\partial\left(n_{1\mathrm{d}}v_{1\mathrm{d}}\right)}{\partial y} = 0, \tag{1}$$

$$\frac{\partial u_{1\mathrm{d}}}{\partial t} + u_{1\mathrm{d}}\frac{\partial u_{1\mathrm{d}}}{\partial x} + v_{1\mathrm{d}}\frac{\partial u_{1\mathrm{d}}}{\partial y} + 3T_{1\mathrm{d(i)}}n_{1\mathrm{d}}\frac{\partial n_{1\mathrm{d}}}{\partial x} = \frac{\partial \phi}{\partial x}, \tag{2}$$

$$\frac{\partial v_{1\mathrm{d}}}{\partial t} + u_{1\mathrm{d}}\frac{\partial v_{1\mathrm{d}}}{\partial x} + v_{1\mathrm{d}}\frac{\partial v_{1\mathrm{d}}}{\partial y} + 3T_{1\mathrm{d(i)}}n_{1\mathrm{d}}\frac{\partial n_{1\mathrm{d}}}{\partial y} = \frac{\partial \phi}{\partial y}, \tag{3}$$

$$\frac{\partial n_{2\mathrm{d}}}{\partial t} + \frac{\partial\left(n_{2\mathrm{d}}u_{2\mathrm{d}}\right)}{\partial x} + \frac{\partial\left(n_{2\mathrm{d}}v_{2\mathrm{d}}\right)}{\partial y} = 0, \tag{4}$$

$$\frac{\partial u_{2\mathrm{d}}}{\partial t} + u_{2\mathrm{d}}\frac{\partial u_{2\mathrm{d}}}{\partial x} + v_{2\mathrm{d}}\frac{\partial u_{2\mathrm{d}}}{\partial y} + 3T_{2\mathrm{d(i)}}n_{2\mathrm{d}}\frac{\partial n_{2\mathrm{d}}}{\partial x} = -ZM_{1\mathrm{d(2d)}}\frac{\partial \phi}{\partial x}, \tag{5}$$

$$\frac{\partial v_{2\mathrm{d}}}{\partial t} + u_{2\mathrm{d}}\frac{\partial v_{2\mathrm{d}}}{\partial x} + v_{2\mathrm{d}}\frac{\partial v_{2\mathrm{d}}}{\partial y} + 3T_{2\mathrm{d(i)}}n_{2\mathrm{d}}\frac{\partial n_{2\mathrm{d}}}{\partial y} = -ZM_{1\mathrm{d(2d)}}\frac{\partial \phi}{\partial y}, \tag{6}$$

$$\frac{\partial^2 \phi}{\partial x^2} + \frac{\partial^2 \phi}{\partial y^2} = \left(n_{\mathrm{i(1d)}} + \beta - 1\right)n_{\mathrm{e}} + n_{1\mathrm{d}} - n_{\mathrm{i(1d)}}n_{\mathrm{i}} - Zn_{2\mathrm{d(1d)}}n_{2\mathrm{d}}, \tag{7}$$

where $n_{1\mathrm{d}}$ ($n_{2\mathrm{d}}$) is the negatively (positively) charged massive dust number density normalized by its equilibrium value $n_{1\mathrm{d}0}$ ($n_{2\mathrm{d}0}$); x and y are space coordinates and are normalized by the Debye length $\lambda_{\mathrm{D(1d)}} = \sqrt{T_{\mathrm{i}}/4\pi Z_{1\mathrm{d}}\mathrm{e}^2 n_{1\mathrm{d}}}$, and the time coordinate is normalized by $\omega_{\mathrm{p(1d)}}^{-1} = \sqrt{m_{1\mathrm{d}}/4\pi Z_{1\mathrm{d}}^2\mathrm{e}^2 n_{1\mathrm{d}}}$; $u_{1\mathrm{d}}$ ($u_{2\mathrm{d}}$) and $v_{1\mathrm{d}}$ ($v_{2\mathrm{d}}$) are the negative (positive) charged dust speed in x and y directions, respectively, and normalized by $C_1 = \sqrt{Z_{1\mathrm{d}}T_{\mathrm{i}}/m_{1\mathrm{d}}}$; ϕ is the electrostatic poten-

tial and normalized by $T_{\rm i}/e$; $T_{\rm 1d}$ ($T_{\rm 2d}$), $T_{\rm i}$, and $T_{\rm e}$ represent the temperature of negatively (positively) charged dusts, isothermal ions, and kappa distributed electrons, respectively; $T_{\rm 1d\,(i)}=T_{\rm 1d}/Z_{\rm 1d}T_{\rm i}$, $T_{\rm 2d\,(i)}=T_{\rm 2d}m_{\rm 1d}/(Z_{\rm 1d}T_{\rm id}m_{\rm 2d})$, $Z=Z_{\rm 2d}/Z_{\rm 1d}$, $M_{\rm 1d\,(2d)}=m_{\rm 1d}/m_{\rm 2d}$, $n_{\rm 2d\,(1d)}=n_{\rm 2d0}/n_{\rm 1d0}$, $n_{\rm i\,(1d)}=n_{\rm i0}/Z_{\rm 1d}n_{\rm 1d0}$, and $T_{\rm i\,(e)}=T_{\rm i}/T_{\rm e}$, with the kappa distributed electrons being expressed as

$$n_{\rm e}=\left[1-\frac{T_{\rm i\,(e)}\phi}{(\kappa_{\rm e}-3/2)}\right]^{-(\kappa_{\rm e}-1/2)}=1+a_1T_{\rm i\,(e)}\phi+a_2T_{\rm i\,(e)}^2\phi^2+a_2T_{\rm i\,(e)}^3\phi^3+\cdots, \tag{8}$$

and the Maxwellian ions as

$$\mathrm{e}^{-\phi}=1-\phi+\phi^2/2-\phi^2/6+\cdots. \tag{9}$$

Inserting Eqs. (8) and (9) into Eq. (7) and then taking up to the third-order terms of ϕ, one can obtain

$$\frac{\partial^2\phi}{\partial x^2}+\frac{\partial^2\phi}{\partial y^2}=\left(Zn_{\rm 2d\,(1d)}-1\right)+n_{\rm 1d}-Zn_{\rm 2d\,(1d)}n_{\rm 2d}+b_1\phi+b_2\phi^2+b_3\phi^3+\cdots, \tag{10}$$

where

$$\begin{aligned}
b_1&=a_1T_{\rm i\,(e)}\left(n_{\rm i\,(1d)}+Zn_{\rm 2d\,(1d)}-1\right)+n_{\rm i\,(1d)},\\
b_2&=a_2T_{\rm i\,(e)}^2\left(n_{\rm i\,(1d)}+Zn_{\rm 2d\,(1d)}-1\right)-n_{\rm i\,(1d)}/2,\\
b_3&=a_3T_{\rm i\,(e)}^3\left(n_{\rm i\,(1d)}+Zn_{\rm 2d\,(1d)}-1\right)+n_{\rm i\,(1d)}/6,\\
a_1&=(\kappa_{\rm e}-1/2)/(\kappa_{\rm e}-3/2),\\
a_2&=(\kappa_{\rm e}-1/2)(\kappa_{\rm e}+1/2)/2(\kappa_{\rm e}-3/2)^2,\\
a_3&=(\kappa_{\rm e}-1/2)(\kappa_{e}+1/2)(\kappa_{\rm e}+3/2)/6(\kappa_{\rm e}-3/2)^3.
\end{aligned}$$

It is noted that $\kappa_{\rm e}>3/2$. In the limit $\kappa_{\rm e}\to\infty$, the kappa distributed electrons become Maxwellian. As a result, the kappa distributed effective thermal speed of electrons approaches to the Maxwellian distributed thermal speed.

3. Derivation of evolution equations and analytical solution with phase shifts

The two-sided Korteweg–de Vries (KdV) equations (KdVEs) are derived by employing ePLK perturbation method to investigate the oblique interaction phenomena of DA waves along with their phase shifts after oblique collision. Accordingly, the expansion of stretched coordinates and perturbed quantities can be considered[46] as

$$\xi=\varepsilon\left(l_1x+m_1y-v_{\rm ph\,\xi}t\right)+\varepsilon^2P_0(\eta,\tau)+\varepsilon^3P_1(\xi,\eta,\tau)+\cdots, \tag{11a}$$

$$\eta=\varepsilon\left(l_2x+m_2y-v_{\rm ph\,\eta}t\right)+\varepsilon^2Q_0(\xi,\tau)+\varepsilon^3Q_1(\xi,\eta,\tau)+\cdots \tag{11b}$$

with $\tau=\varepsilon^3t$, and

$$n_{\rm 1d}=1+\varepsilon^2n_{\rm 1d}^{(1)}+\varepsilon^4n_{\rm 1d}^{(2)}+\varepsilon^6n_{\rm 1d}^{(3)}+\cdots, \tag{12a}$$

$$n_{\rm 2d}=1+\varepsilon^2n_{\rm 2d}^{(1)}+\varepsilon^4n_{\rm 2d}^{(2)}+\varepsilon^6n_{\rm 2d}^{(3)}+\cdots, \tag{12b}$$

$$u_{\rm 1d}=0+\varepsilon^2u_{\rm 1d}^{(1)}+\varepsilon^4u_{\rm 1d}^{(2)}+\varepsilon^6u_{\rm 1d}^{(3)}+\cdots, \tag{12c}$$

$$v_{\rm 1d}=0+\varepsilon^2v_{\rm 1d}^{(1)}+\varepsilon^4v_{\rm 1d}^{(2)}+\varepsilon^6v_{\rm 1d}^{(3)}+\cdots, \tag{12d}$$

$$u_{\rm 2d}=0+\varepsilon^2u_{\rm 2d}^{(1)}+\varepsilon^4u_{\rm 2d}^{(2)}+\varepsilon^6u_{\rm 2d}^{(3)}+\cdots, \tag{12e}$$

$$v_{\rm 2d}=0+\varepsilon^2v_{\rm 2d}^{(1)}+\varepsilon^4v_{\rm 2d}^{(2)}+\varepsilon^6v_{\rm 2d}^{(3)}+\cdots, \tag{12f}$$

$$\phi=0+\varepsilon^2\phi^{(1)}+\varepsilon^4\phi^{(2)}+\varepsilon^6\phi^{(3)}+\cdots, \tag{12g}$$

where ε is the small quantity ($0<\varepsilon<1$) for measuring the strength of nonlinearity, ξ and η represent the trajectories of two DA waves propagating in $\boldsymbol{r}_1=(l_1,m_1)$ and $\boldsymbol{r}_2=(l_2,m_2)$ directions, respectively, $\boldsymbol{r}_1\cdot\boldsymbol{r}_2=l_1l_2+m_1m_2$ and the collision angle can be obtained from

$$\cos\theta=(l_1l_2+m_1m_2)/\left(l_2^2+m_2^2\right)^{1/2}\left(l_2^2+m_2^2\right)^{1/2}=\lambda/\lambda_1\lambda_2,$$

where

$$\lambda=l_1l_2+m_1m_2,\ \lambda_1=\left(l_1^2+m_1^2\right)^{1/2},\ \lambda_2=\left(l_2^2+m_2^2\right)^{1/2}.$$

The phase velocities $v_{\rm ph\,\xi}$, and $v_{\rm ph\,\eta}$ of DA waves, and the variables $P_0(\eta,\tau)$ and $Q_0(\xi,\tau)$ will be determined latter. Equations (11a) and (11b) yield the following operators

$$\frac{\partial}{\partial t}\equiv-\varepsilon\left(v_{\rm ph}\frac{\partial}{\partial\xi}+v_{\rm ph}\frac{\partial}{\partial\eta}\right)-\varepsilon^3\left(\frac{\partial P_0}{\partial\eta}\frac{\partial}{\partial\xi}+\frac{\partial Q_0}{\partial\xi}\frac{\partial}{\partial\eta}\right)+\varepsilon^3\frac{\partial}{\partial\tau}+\cdots, \tag{13a}$$

$$\frac{\partial}{\partial x}\equiv\varepsilon\left(l_1\frac{\partial}{\partial\xi}+l_2\frac{\partial}{\partial\eta}\right)+\varepsilon^3\left(l_2\frac{\partial P_0}{\partial\eta}\frac{\partial}{\partial\xi}+l_1\frac{\partial Q_0}{\partial\xi}\frac{\partial}{\partial\eta}\right)+\cdots, \tag{13b}$$

$$\frac{\partial}{\partial y}\equiv\varepsilon\left(m_1\frac{\partial}{\partial\xi}+m_2\frac{\partial}{\partial\eta}\right)+\varepsilon^3\left(m_2\frac{\partial P_0}{\partial\eta}\frac{\partial}{\partial\xi}+m_1\frac{\partial Q_0}{\partial\xi}\frac{\partial}{\partial\eta}\right)+\cdots. \tag{13c}$$

Inserting Eqs. (12a)–(12g) and (13a)–(13c) into Eqs. (1)–(6) and (10), one can obtain a set of partial differential equations (PDEs) in powers of ε. Collecting the terms having equal powers of ε, the leading (smallest) order of ε yields a system of PDEs (see expressions (A1) in Appendix A.

Solving expressions (A1) in Appendix A, one can obtain the following relations:

$$\phi^{(1)}=\phi_\xi^{(1)}+\phi_\eta^{(1)}, \tag{14a}$$

$$n_{\rm 1d}^{(1)}=\bar{a}_1\phi_\xi^{(1)}+\bar{b}_1\phi_\eta^{(1)}, \tag{14b}$$

$$u_{\rm 1d}^{(1)}=\bar{a}_2\phi_\xi^{(1)}+\bar{b}_2\phi_\eta^{(1)}, \tag{14c}$$

$$v_{\rm 1d}^{(1)}=\bar{a}_3\phi_\xi^{(1)}+\bar{b}_3\phi_\eta^{(1)}, \tag{14d}$$

$$n_{\rm 2d}^{(1)}=-\left[c_1\phi_\xi^{(1)}+\bar{c}_1\phi_\eta^{(1)}\right], \tag{14e}$$

$$u_{\rm 2d}^{(1)}=-\left[c_2\phi_\xi^{(1)}+\bar{c}_2\phi_\eta^{(1)}\right], \tag{14f}$$

$$v_{\rm 2d}^{(1)}=-\left[c_3\phi_\xi^{(1)}+\bar{c}_3\phi_\eta^{(1)}\right]. \tag{14g}$$

The phase velocities can be obtained to be

$$v_{\mathrm{ph}\,\xi}^4 - \lambda_1^2\left[\left(1+3T_{1\mathrm{d}\,(\mathrm{i})}\right)+Z^2M_{1\mathrm{d}\,(2\mathrm{d})}n_{2\mathrm{d}\,(1\mathrm{d})}\right]v_{\mathrm{ph}\,\xi}^2+3\lambda_1^4\left[Z^2M_{1\mathrm{d}\,(2\mathrm{d})}n_{2\mathrm{d}\,(1\mathrm{d})}T_{1\mathrm{d}\,(\mathrm{i})}+T_{2\mathrm{d}\,(\mathrm{i})}+3b_1T_{1\mathrm{d}\,(\mathrm{i})}T_{2\mathrm{d}\,(\mathrm{i})}\right]=0, \quad (15)$$

$$v_{\mathrm{ph}\,\eta}^4 - \lambda_2^2\left[\left(1+3T_{1\mathrm{d}\,(\mathrm{i})}\right)+Z^2M_{1\mathrm{d}\,(2\mathrm{d})}n_{2\mathrm{d}\,(1\mathrm{d})}\right]v_{\mathrm{ph}\,\eta}^2+3\lambda_2^4\left[Z^2M_{1\mathrm{d}\,(2\mathrm{d})}n_{2\mathrm{d}\,(1\mathrm{d})}T_{1\mathrm{d}\,(\mathrm{i})}+T_{2\mathrm{d}\,(\mathrm{i})}+3b_1T_{1\mathrm{d}\,(\mathrm{i})}T_{2\mathrm{d}\,(\mathrm{i})}\right]=0, \quad (16)$$

where $\phi_\xi^{(1)}(\xi,\tau)\approx\phi_\xi^{(1)}$, $\phi_\eta^{(1)}(\eta,\tau)\approx\phi_\eta^{(1)}$, and $\bar{a}_1$, $\bar{a}_2$, $\bar{a}_3$, $\bar{b}_1$, $\bar{b}_2$, $\bar{b}_3c_1$, c_2c_3, $\bar{c}_1$, $\bar{c}_2$, and $\bar{c}_3$ are presented in Appendix (A2).

The next higher power of ε provides a set of PDEs and then after some algebraic manipulations and using Eqs. (14a)–(14g), one can find

$$\frac{1}{2}\frac{\partial\Lambda}{\partial\xi\partial\eta}=\frac{\partial}{\partial\xi}\left[\frac{\partial\phi_\xi^{(1)}}{\partial\tau}+C_{1\mathrm{N}}\phi_\xi^{(1)}\frac{\partial\phi_\xi^{(1)}}{\partial\xi}+C_{1\mathrm{D}}\frac{\partial^3\phi_\xi^{(1)}}{\partial\xi^3}\right]+\frac{\partial}{\partial\eta}\left[\frac{\partial\phi_\eta^{(1)}}{\partial\tau}+C_{2\mathrm{N}}\phi_\eta^{(1)}\frac{\partial\phi_\eta^{(1)}}{\partial\eta}+C_{2\mathrm{D}}\frac{\partial^3\phi_\eta^{(1)}}{\partial\eta^3}\right]$$
$$+\left[L\phi_\eta^{(1)}-M\frac{\partial P_0}{\partial\eta}\right]\frac{\partial^2\phi_\xi^{(1)}}{\partial\xi^2}+\left[L_1\phi_\xi^{(1)}-M_1\frac{\partial Q_0}{\partial\xi}\right]\frac{\partial^2\phi_\eta^{(1)}}{\partial\eta^2}, \quad (17)$$

where $C_{1\mathrm{N}}$ and $C_{2\mathrm{N}}$ ($C_{1\mathrm{D}}$, $C_{2\mathrm{D}}$) are the coefficients of nonlinearity (dispersion) of the DA waves (Appendix (A3)), $\Lambda=Xu_{1\mathrm{d}}^{(2)}+Yv_{1\mathrm{d}}^{(2)}+\bar{X}u_{2\mathrm{d}}^{(2)}+\bar{Y}v_{2\mathrm{d}}^{(2)}$.

Integrating Eq. (17) with respect to ξ and η, respectively, one can obtain

$$\frac{1}{2}\Lambda=\int\left[\frac{\partial\phi_\xi^{(1)}}{\partial\tau}+C_{1\mathrm{N}}\phi_\xi^{(1)}\frac{\partial\phi_\xi^{(1)}}{\partial\xi}+C_{1\mathrm{D}}\frac{\partial^3\phi_\xi^{(1)}}{\partial\xi^3}\right]\mathrm{d}\eta+\int\left[\frac{\partial\phi_\eta^{(1)}}{\partial\tau}+C_{2\mathrm{N}}\phi_\eta^{(1)}\frac{\partial\phi_\eta^{(1)}}{\partial\eta}+C_{2\mathrm{D}}\frac{\partial^3\phi_\eta^{(1)}}{\partial\eta^3}\right]\mathrm{d}\xi$$
$$+\iint\left[L\phi_\eta^{(1)}-M\frac{\partial P_0}{\partial\eta}\right]\frac{\partial^2\phi_\xi^{(1)}}{\partial\xi^2}\mathrm{d}\xi\,\mathrm{d}\eta+\iint\left[L_1\phi_\xi^{(1)}-M_1\frac{\partial Q_0}{\partial\xi}\right]\frac{\partial^2\phi_\eta^{(1)}}{\partial\eta^2}\mathrm{d}\xi\,\mathrm{d}\eta. \quad (18)$$

The first and second terms in the integrands on the right-hand side of Eq. (18) are proportional to η and ξ, respectively, for these are independent of η and ξ. Each term of the first and second expressions on the right-hand side of Eq. (18) become secular and these can be eliminated in order to avoid spurious resonances. Thus, the well-known two-sided KdVEs can be obtained from Eq. (18) to be

$$\frac{\partial\phi_\xi^{(1)}}{\partial\tau}+C_{1\mathrm{N}}\phi_\xi^{(1)}\frac{\partial\phi_\xi^{(1)}}{\partial\xi}+C_{1\mathrm{D}}\frac{\partial^3\phi_\xi^{(1)}}{\partial\xi^3}=0, \quad (19)$$

$$\frac{\partial\phi_\eta^{(1)}}{\partial\tau}+C_{2\mathrm{N}}\phi_\eta^{(1)}\frac{\partial\phi_\eta^{(1)}}{\partial\eta}+C_{2\mathrm{D}}\frac{\partial^3\phi_\eta^{(1)}}{\partial\eta^3}=0. \quad (20)$$

The third and fourth terms in the right-hand side of Eq. (18) are not secular, thus, the next higher order of ε would be secular and yields

$$\frac{\partial P_0}{\partial\eta}=\frac{L}{M}\phi_\eta^{(1)},\quad \frac{\partial Q_0}{\partial\xi}=\frac{L_1}{M_1}\phi_\xi^{(1)}. \quad (21)$$

The principal phase functions P_0 and Q_0 can be estimated by solving Eq. (21) with the help of analytical solutions of KdVEs (Eqs. (19) and (20)). It is noted that Eqs. (19) and (20) characterize the two-sided travelling waves in the reference frames ξ and η, respectively. The solutions of KdVEs (Eqs. (19) and (20) can be obtained to be

$$\phi_\xi^{(1)}=\varphi_{\xi0}\,\mathrm{sech}^2\left(\frac{\chi}{W_\xi}\right), \quad (22)$$

$$\phi_\eta^{(1)}=\varphi_{\eta0}\,\mathrm{sech}^2\left(\frac{\chi_1}{W_\eta}\right). \quad (23)$$

Here, $\chi=\xi-U_0\tau$, $\chi_1=\eta+U_0\tau$, and $\varphi_{\xi0}=3U_0/C_{1\mathrm{N}}$ $\left(W_\xi=\sqrt{4C_{1\mathrm{D}}/U_0}\right)$ are the amplitudes (width) of the right traveling solitons and $\varphi_{\eta0}=3U_0/C_{2\mathrm{N}}$ $\left(W_\eta=\sqrt{4C_{2\mathrm{D}}/U_0}\right)$ is the amplitude (width) of the left traveling solitons at their initial positions, U_0 being the constant velocity of the solitons. To determine the phase shifts due to head-on collision between two solitons say S_ξ (S_η) traveling toward right (left) direction, it is assumed that initially ($t\to-\infty$)S_ξ at $\xi=0$, $\eta\to-\infty$, and S_η at $\eta=0$, $\xi\to+\infty$ are asymptotically away from each other. After some time they will collide and then depart. That is, after collision S_ξ will be at $\xi=0$, $\eta\to+\infty$ and S_η will be at $\eta=0$, $\xi\to-\infty$. The phase shifts can be determined from the solutions (Eqs. (22) and (23)) of KdVEs along with Eq. (21) to be

$$\Delta\delta_\eta=-2\varepsilon^2\frac{L}{M}\varphi_{\eta0}W_\eta,$$
$$\Delta\delta_\xi=2\varepsilon^2\frac{L_1}{M_1}\varphi_{\xi0}W_\xi. \quad (24)$$

4. Results and discussion

The un-magnetized dusty plasma consisting of inertial warm negatively charged massive dusts, positively charged dusts, superthermal kappa distributed electrons and isothermal ions as observed in space mentioned earlier, is considered to investigate the oblique interaction phenomena of DA

waves. In this regard, the ePLK method is used to derive the two-sided KdVEs. The KdV-like soliton solutions presented in Eqs. (22) and (23) are existent due to the balance between nonlinearity (C_{1N} and C_{2N}) and dispersion (C_{1D} and C_{2D}). So, if $C_{1N}C_{1D}$ $(C_{2N}C_{2D}) > 0$ and both $\varphi_{\xi 0}$ and $\varphi_{\eta 0}$ are positive, the KdV solitons are obtained from Eqs. (19) and (20) and known as compressive DA wave solitons. Besides, the KdV soliton obtained is called rarefactive DA wave soliton, while $C_{1N}C_{1D}$ $(C_{2N}C_{2D}) < 0$ and both $\varphi_{\xi 0}$ and $\varphi_{\eta 0}$ are negative. As it is assumed that the solitons S_ξ and S_η travel toward right and left directions, respectively, therefore, one can see from Eq. (24) that each soliton has a phase shift due to collision in their respective direction of propagation. The plasma parameters are considered here in this work as follows: $M_{1d(2d)} = m_{1d}/m_{2d} = 150$, $n_{2d(1d)} = n_{2d0}/n_{1d0} = 0.1$, $n_{i(1d)} = n_{10}/Z_{1d}n_{1d0} = 0.1$–$0.6$, $T_{i(e)} = T_i/T_e = 0.1$–0.3, $T_{1d(i)} = T_{1d}/Z_{1d}T_i = 10^{-5}$, $T_{2d(i)} = T_{1d}m_{1d}/m_{2d}Z_{1d}T_i = 10^{-4}$, $Z_{2d}/Z_{1d} = 0.01$–0.09, $\kappa_e = 2.0$–2.6, and the remaining parameters are all constant. The head-on collisional dynamics of DA waves for KdV solitons are displayed in Fig. 1 with velocities $v_{ph\xi} = 0.045$ and $v_{ph\eta} = 0.45$, but they travel in opposite directions with the obliqueness θ. In Fig. 1, panels 1(b) and 1(d) represent the contour of the panels 1(a) and 1(c), while panels 1(a) and 1(c) show the colisional effects at $\theta = 30°$ and $\theta = 45°$, respectively. These figures reveal the formation of new nonlinear wave structures in the colliding region, which is in good agreement with the finding of El-Shamy *et al.*[54] Besides, the pronounced soliton structures are produced for small obliqueness. Figure 2(a) (for $\theta = 45°$) is the 2D plot of Fig. 1(b), while figure 2(b) is the 2D plot of Fig. 1(a).

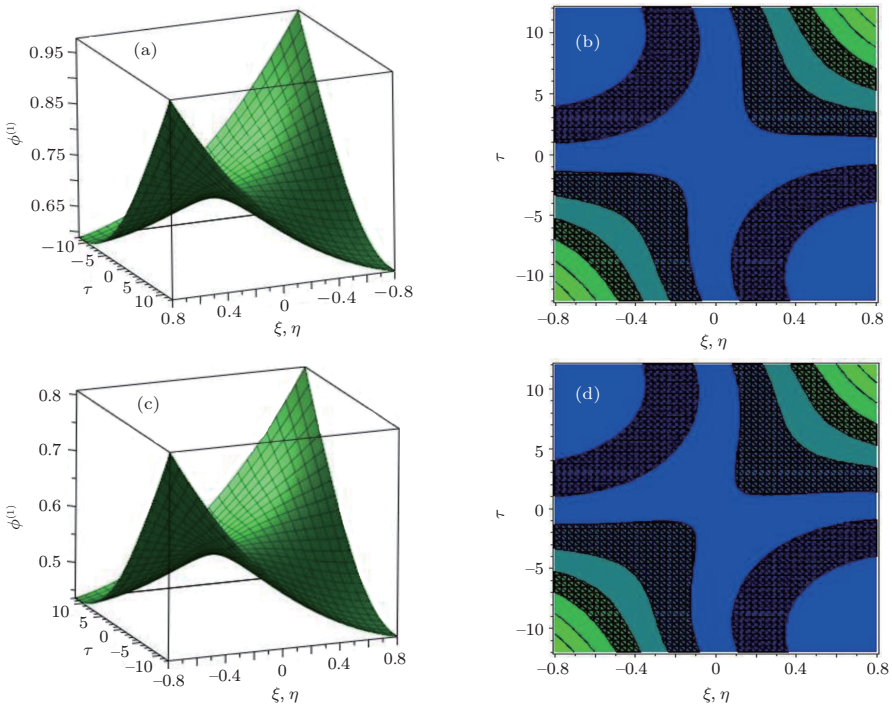


Fig. 1. Oblique colisional effects of dust acoustic waves on electrostatic potential $\phi^{(1)} = \phi_\xi^{(1)} + \phi_\eta^{(1)}$ for $\theta = 30°$ (a) and $\theta = 45°$ (c) with $n_{2d(1d)} = 0.1$, $n_{i(1d)} = 0.4$, $Z = 0.01$, $T_{1d(i)} = 10^{-5}$, $T_{2d(i)} = 10^{-4}$, $\kappa_e = 3$, $T_{i(e)} = 0.1$, $v_{ph\xi} = 0.045$, $v_{ph\eta} = 0.045$, $M_{1d(2d)} = 150$, and $U_0 = 0.09$. Panels (b) and (d) are contour plots of panels (a) and (c).

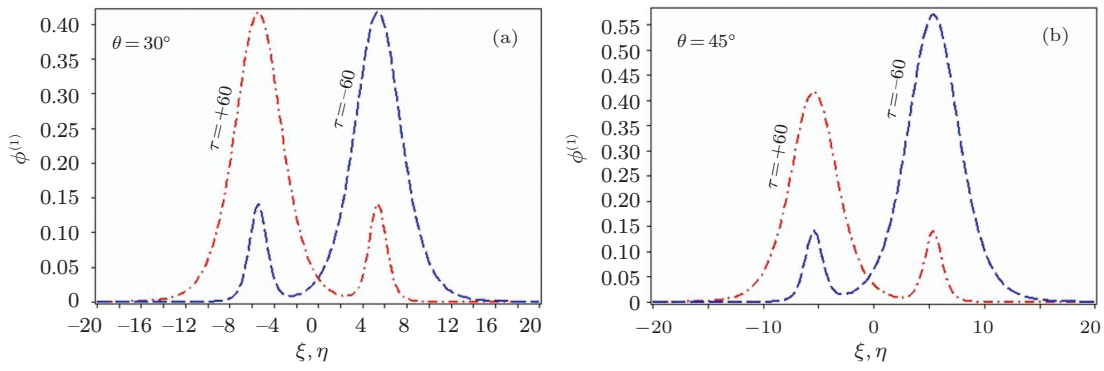


Fig. 2. Oblique colisional effects of dust acoustic waves on electrostatic potential $\phi^{(1)} = \phi_\xi^{(1)} + \phi_\eta^{(1)}$ for $\theta = 45°$ (a) and $\theta = 30°$ (b) with $n_{2d(1d)} = 0.1$, $n_{i(1d)} = 0.4$, $Z = 0.01$, $T_{1d(i)} = 10^{-5}$, $T_{2d(i)} = 10^{-4}$, $\kappa_e = 3$, $T_{i(e)} = 0.1$, $v_{ph\xi} = 0.045$, $v_{ph\eta} = 0.045$, $M_{1d(2d)} = 150$, and $U_0 = 0.09$.

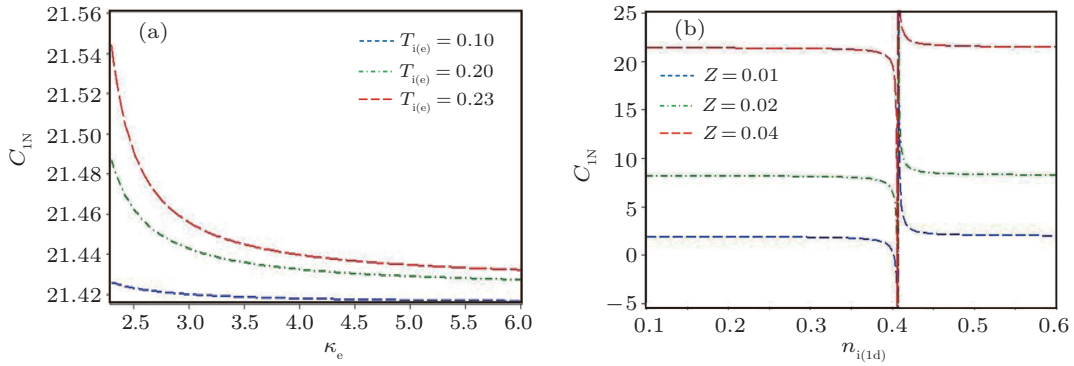


Fig. 3. Oblique colisional effects of dust acoustic waves on nonlinear coefficients C_{1N} of rightward traveling KdV solitons for (a) $T_{i(e)}$ taking with $n_{2d(1d)} = 0.1$, $n_{i(1d)} = 0.4$, $Z = 0.04$, $T_{1d(i)} = 10^{-5}$, $T_{2d(i)} = 10^{-4}$, $v_{ph\xi} = 0.045$, $v_{ph\eta} = 0.045$, $M_{1d(2d)} = 150$, $\theta = 45^\circ$ and $U_0 = 0.09$; (b) Z taking with $\kappa_e = 2$, $T_{i(e)} = 0.1$, and the remaining parameters are the same as those in Fig. 1(a).

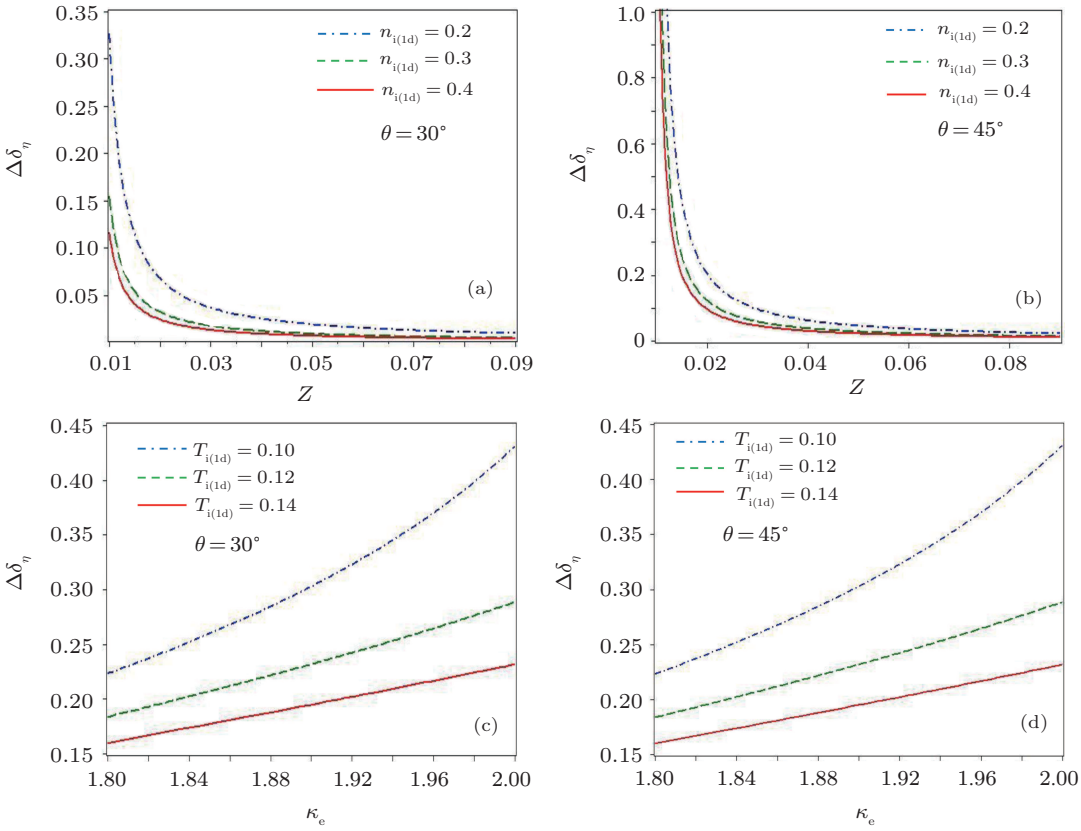


Fig. 4. Effects on phase shift $\Delta\delta_\eta$ for (a) $n_{i(1d)}$ taking with $\theta = 30^\circ$, $n_{2d(1d)} = 0.1$, $n_{i(1d)} = 0.4$, $T_{1d(i)} = 10^{-5}$, $T_{2d(i)} = 10^{-4}$, $T_{i(e)} = 0.1$, $v_{ph\xi} = 0.045$, $v_{ph\eta} = 0.045$, $M_{1d(2d)} = 150$, $\varepsilon = 0.1$, and $U_0 = 0.09$; (b) $n_{i(1d)}$, $\theta = 45^\circ$ taking with the remaining parameters being the same as those in Fig. 4(a) with Z; (c) $T_{i(1d)}$, $\theta = 30^\circ$; and (d) $T_{i(1d)}$, $\theta = 45^\circ$ taking with the remaining parameters being the same as those in Fig. 4(a) with κ_e.

The effect on nonlinear coefficient (C_{1N}) with κ_e for $T_{i(e)}$ is displayed in Fig. 3(a) and revels the enhancement of C_{1N} with the increase of $T_{i(e)}$ of the DA wave solitons. Further, the decreasing rate of C_{1N} becomes larger in a lower range of κ_e ($\kappa_e < 3.5$) than that for a higher range of κ_e ($\kappa_e \geq 3.5$). The effect of $n_{i(1d)}$ on C_{1N} with Z is described in Fig. 3(b) and it is shown that C_{1N} is increasing with Z of the DA wave solitons increasing, but no effect on $n_{i(1d)}$ is observed except in the critical region, while C_{1N} is decreasing due to the increase of $n_{i(1d)}$ around the critical region. The driving force (provided by the inertia of n_{1d}) is decreasing due to the depopulation of n_{1d} around the critical region ($n_{i(1d)} = 0.46$), consequently the nonlinearity of DA waves decreases with $n_{i(1d)}$ increasing.

It is mentioned earlier that the solitons S_ξ and S_η travel toward the right and left direction, respectively. Therefore, one can see from Eq. (24) that each soliton produces a phase shift due to collision in its direction of propagation. The phase shifts of the solitons are produced due to gaining energy from the medium preserving their original shapes. The phase shifts are produced due to head-on collisions between the two counter-propagating solitons. They may be either positive or negative depending on the sign of L/M or L_1/M_1 (Eq. (24)). Figures 4(a) ($\theta = 30^\circ$) and 4(b) ($\theta = 45^\circ$) successively show the effect of Z with $n_{i(1d)}$ on the phase shift. These figures

show that the phase shifts decrease with both $n_{i(1d)}$ and Z increasing. It is noted that the phase shifts become pronounced with both $n_{i(1d)}$ and Z decreasing. Thus, obliqueness plays a crucial role in changing phase shift. Figures 4(c) ($\theta = 30°$) and 4(d) ($\theta = 45°$) show the effect of κ_e with $T_{i(e)}$ on phase shift. It is observed that the phase shift decreasing with $T_{i(e)}$ increasing, while it increases almost linearly with κ_e increasing. It is also noted that the decreasing rate of phase shift becomes more pronounced for small values of $T_{i(e)}$. The effects of obliqueness on the phase shift are insignificant which can also be observed from Figs. 4(c) and 4(d). Furthermore, it is seen from Fig. 4 that the phase shift is positive in each case, which means that the trajectories of the travelling solitons are slower than those of solitons without collision.

Figures 5(a) and 5(b) show the effects of obliqueness and temperature ratio of isothermal ion to electron ($T_{i(e)}$) on amplitudes of the DA wave solitons, respectively. Figure 5(a) displays that the amplitude increases with both θ and κ_e increasing. This can be explained as the fact that the coefficient of nonlinearity drops down while the dispersive coefficient goes up due to the enhancement of κ_e, consequently the amplitude of soliton increases. Besides, the amplitude decreases with $T_{i(e)}$ increasing, but asymptotically increases with $n_{i(1d)}$ increasing as observed from Fig. 5(b). Due to the enhancement of T_i the loss rate of energy becomes pronounced, as a result the amplitudes decrease. Besides, the restoring force provided by the isothermal ions increases due to the increase in n_i (depopulation of n_{1d}), consequently the amplitude increases with $n_{i(1d)}$ increasing. It is obvious that the amplitudes of the coupled KdV solitons and their corresponding phase shifts obtained from the Eqs. (19) and (20) become infinite while $C_{1N} \to 0$ and $C_{2N} \to 0$ for the critical values of κ_e. One can obtain (for rightward traveling soliton) the critical value of κ_e: $\kappa_{ec} \cong 1.507$ for $C_{1N} = 0$ with the plasma parameters taken as $n_{2d(1d)} = 0.1$, $n_{i(1d)} = 0.4$, $Z = 0.04$, $T_{1d(i)} = 10^{-5}$, $T_{2d(i)} = 10^{-4}$, $T_{i(e)} = 0.1$, $v_{ph\xi} = 0.045$, $v_{ph\eta} = 0.45$, $M_{1d(2d)} = 150$, $\theta = 45°$ and $U_0 = 0.09$. Balance between the nonlinearity and dispersion is the necessary condition for producing the KdV solitons. Thus, for $\kappa_e \cong \kappa_{ec}$, the nonlinearity terms of the coupled KdV equations become zero, consequently it is impossible for KdV solitons to exist. Since the dispersive coefficients (C_{1D} and C_{2D}) are always positive, therefore it is dependent on the signs of nonlinear coefficients (C_{1N} and C_{2N}) that the KdV solitons are either compressive or rarefactive. In the present study for the rightward traveling soliton $C_{1N} \lessgtr 0$ holds, thus the rarefactive and compressive DA soliton structure are formed.

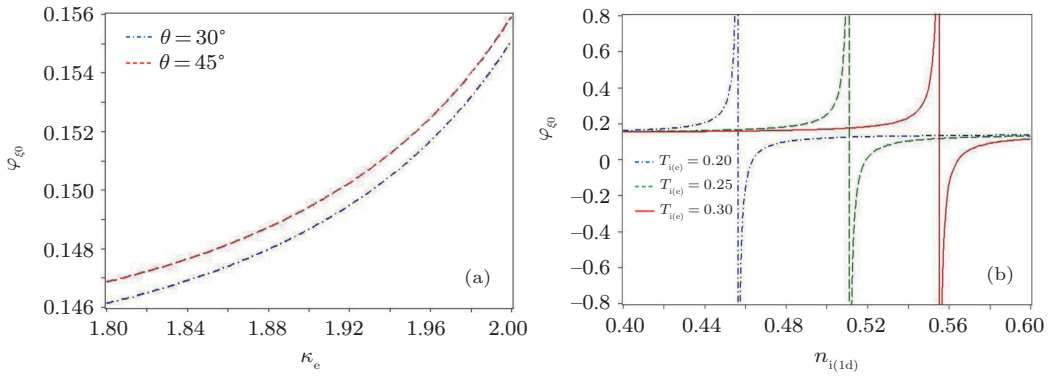


Fig. 5. Variations of amplitude of rightward traveling solitons with (a) κ_e for $\theta = 30°$, $\theta = 45°$ for $n_{2d(1d)} = 0.1$, $n_{i(1d)} = 0.4$, $T_{1d(i)} = 10^{-5}$, $T_{2d(i)} = 10^{-4}$, $T_{i(e)} = 0.1$, $M_{1d(2d)} = 150$, $\varepsilon = 0.1$, and $U_0 = 0.09$; (b) $n_{i(1d)}$ for $\theta = 45°$, $T_{i(e)} = 0.20, 0.25, 0.30$ taking with the remaining parameters being the same as those in Fig. 5(a).

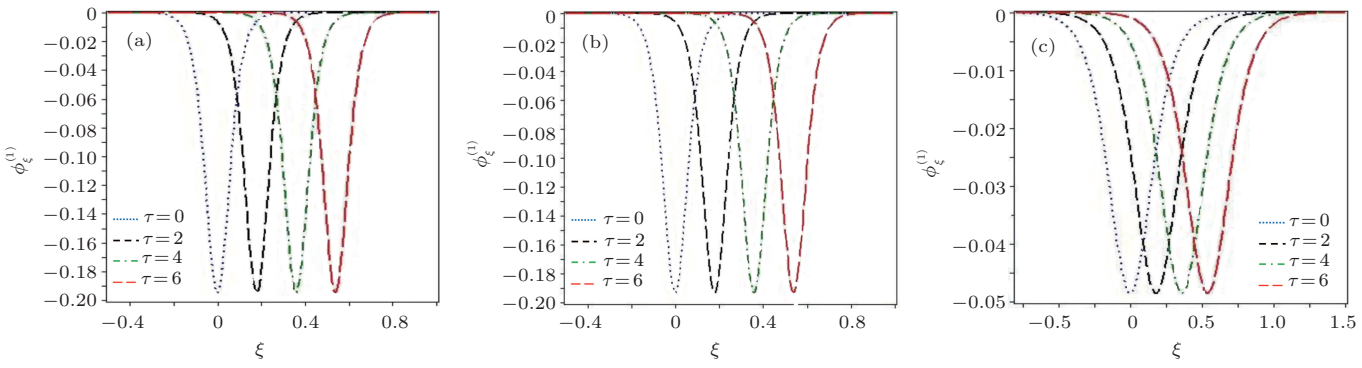


Fig. 6. Effects on structure of potential profile of rightward traveling solitons for (a) $\theta = 30°$, (b) $\theta = 45°$, and (c) $\theta = 75°$, with parameters taking as $\kappa_e = 1.504$, $n_{2d(1d)} = 0.1$, $n_{i(1d)} = 0.2$, $Z = 0.01$, $T_{1d(i)} = 10^{-5}$, $T_{2d(i)} = 10^{-4}$, $T_{i(e)} = 0.3$, $v_{ph\xi} = 0.045$, $v_{ph\eta} = 0.045$, $M_{1d(2d)} = 150$, $\varepsilon = 0.1$, and $U_0 = 0.09$.

Figures 6(a)–6(c) show the effects of θ for $\kappa_e < \kappa_{ec}$ on the rightward travelling solitons due to oblique collisions. Figures 6(a)–6(c) explain the effects of $\theta = 30^\circ$, $\theta = 45^\circ$, and $\theta = 75^\circ$, respectively, for the rightward travelling solitons. One can observe from these figures that the dip shape (rarefactive) structures of the potential profiles are formed in each case of obliqueness. Thus, the structures of potential profiles become pronounced for the small values of θ.

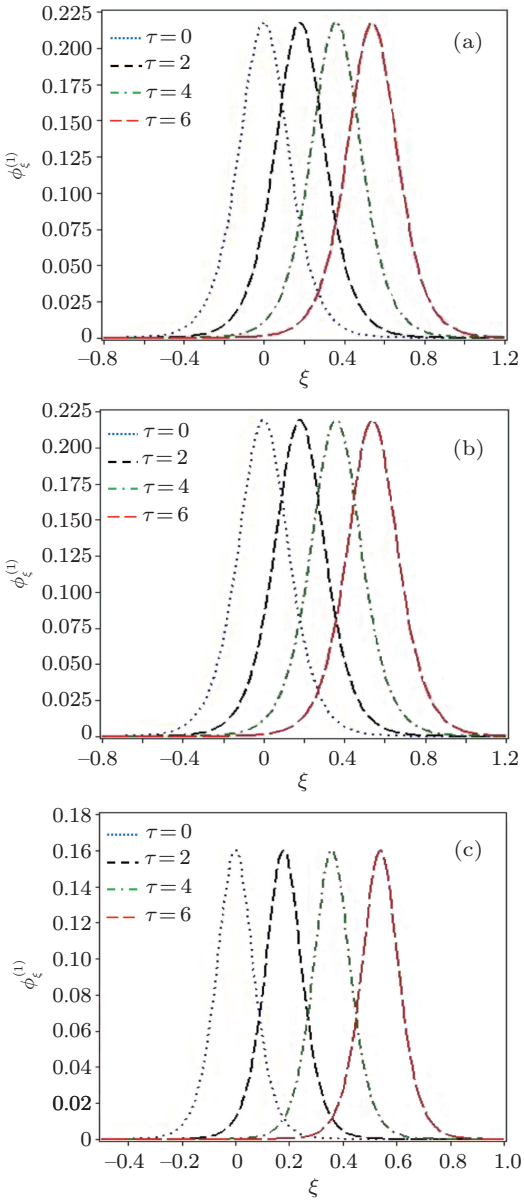


Fig. 7. Effects on structure of potential profile of rightward traveling solitons for (a) $\theta = 30^\circ$, (b) $\theta = 45^\circ$, and (c) $\theta = 75^\circ$, with parameters taking as $\kappa_e = 1.52$, $n_{2d(1d)} = 0.1$, $n_{i(1d)} = 0.2$, $Z = 0.01$, $T_{1d(i)} = 10^{-5}$, $T_{2d(i)} = 10^{-4}$, $T_{i(e)} = 0.3$, $v_{ph\xi} = 0.045$, $v_{ph\eta} = 0.045$, $M_{1d(2d)} = 150$, $\varepsilon = 0.1$, and $U_0 = 0.09$.

Figures 7(a)–7(c) display the effects of obliqueness ($\theta = 30^\circ$, $\theta = 45^\circ$, and $\theta = 75^\circ$) for $\kappa_e > \kappa_{ec}$ on the structures of the potential profiles for the rightward travelling solitons due to oblique collision. These figures reveal that the humpshaped (compressive) soliton is produced in each case due to the effect of obliqueness θ and that the largest amplitude of soliton is produced for small θ. Besides, figures 6 and 7 expose that the smallest value of obliqueness is prominent and the soliton propagates from left to right direction with time, which is in good agreement with analytical result.[55,56] Finally, the rarefactive (compressive) soliton structure is formed for $\kappa_e < \kappa_{ec}$ ($\kappa_e > \kappa_{ec}$).

5. Summary

The fully ionized un-magnetized dusty plasma is considered to investigate the oblique interaction phenomena of the DA waves. The plasma system consists of inertial warm negatively charged massive dusts, positively charged dusts, superthermal kappa distributed electrons, and isothermal ions. The KdVEs are derived by employing the ePLK method. The important results obtained in this paper are summed up as follows. New nonlinear wave structures are formed in the colliding region due to the head-on collision of the two counter propagating DA waves that depend on the degree of obliqueness. Near the critical value of $n_{i(1d)}$ ($n_{i(1d)} = 0.46$), the nonlinearity decreases with $n_{i(1d)}$ increasing. The phase shifts decrease (increase) with $T_{i(e)}$ (κ_e) increasing. The humpshaped (compressive) and dipshaped (rarefactive) solitons are produced depending on θ for $\kappa_e < \kappa_{ec}$ and $\kappa_e > \kappa_{ec}$, respectively. The proposed model may be useful for explaining the results for both space (such as, lower and upper mesospheres, cometary tails, planetary rings, planetary magnetospheres, inter-planetary spaces, interstellar plasma media, *etc*.) and laboratory experiments (*e.g*., Q-machine plasma, RF plasma, microwave plasma, fusion plasma, *etc*.), where the inertial warm negatively charged massive dusts, positively charged dusts, superthermal kappa distributed electrons, and isothermal ions are the combined attribution.

Appendix A

Some partial differential equations and coefficients in deriving the evolution equations and their analytical solutions of our fluid model are given below:

$$-v_{ph\xi}\frac{\partial n_{1d}^{(1)}}{\partial \xi} - v_{ph\xi}\frac{\partial n_{1d}^{(1)}}{\partial \eta} + l_1\frac{\partial u_{1d}^{(1)}}{\partial \xi} + l_2\frac{\partial u_{1d}^{(1)}}{\partial \eta} + m_1\frac{\partial v_{1d}^{(1)}}{\partial \xi} + m_2\frac{\partial v_{1d}^{(1)}}{\partial \eta} = 0,$$

$$-v_{ph\xi}\frac{\partial u_{1d}^{(1)}}{\partial \xi} - v_{ph\xi}\frac{\partial u_{1d}^{(1)}}{\partial \eta} + 3T_{1d(i)}l_1\frac{\partial n_{1d}^{(1)}}{\partial \xi} + 3T_{1d(i)}l_2\frac{\partial n_{1d}^{(1)}}{\partial \eta} - l_1\frac{\partial \phi^{(1)}}{\partial \xi} - l_2\frac{\partial \phi^{(1)}}{\partial \eta} = 0,$$

$$
\begin{aligned}
&-v_{\mathrm{ph}\,\xi}\frac{\partial v_{1\mathrm{d}}^{(1)}}{\partial\xi}-v_{\mathrm{ph}\,\xi}\frac{\partial v_{1\mathrm{d}}^{(1)}}{\partial\eta}+3T_{1d(i)}m_1\frac{\partial n_{1\mathrm{d}}^{(1)}}{\partial\xi}+3T_{1\mathrm{d(i)}}m_2\frac{\partial n_{1\mathrm{d}}^{(1)}}{\partial\eta}-m_1\frac{\partial\phi^{(1)}}{\partial\xi}-m_2\frac{\partial\phi^{(1)}}{\partial\eta}=0,\\
&-v_{\mathrm{ph}\,\xi}\frac{\partial n_{2\mathrm{d}}^{(1)}}{\partial\xi}-v_{\mathrm{ph}\,\xi}\frac{\partial n_{2\mathrm{d}}^{(1)}}{\partial\eta}+l_1\frac{\partial u_{2\mathrm{d}}^{(1)}}{\partial\xi}+l_2\frac{\partial u_{2\mathrm{d}}^{(1)}}{\partial\eta}+m_1\frac{\partial v_{2\mathrm{d}}^{(1)}}{\partial\xi}+m_2\frac{\partial v_{2\mathrm{d}}^{(1)}}{\partial\eta}=0,\\
&-v_{\mathrm{ph}\,\xi}\frac{\partial u_{2\mathrm{d}}^{(1)}}{\partial\xi}-v_{\mathrm{ph}\,\xi}\frac{\partial u_{2\mathrm{d}}^{(1)}}{\partial\eta}+3T_{2d\,(i)}l_1\frac{\partial n_{2\mathrm{d}}^{(1)}}{\partial\xi}+3T_{2\mathrm{d}\,(\mathrm{i})}l_2\frac{\partial n_{2\mathrm{d}}^{(1)}}{\partial\eta}+ZM_{1\mathrm{d}\,(2\mathrm{d})}l_1\frac{\partial\phi^{(1)}}{\partial\xi}+ZM_{1\mathrm{d}\,(2\mathrm{d})}l_2\frac{\partial\phi^{(1)}}{\partial\eta}=0,\\
&-v_{\mathrm{ph}\,\xi}\frac{\partial v_{2\mathrm{d}}^{(1)}}{\partial\xi}-v_{\mathrm{ph}\,\xi}\frac{\partial v_{2\mathrm{d}}^{(1)}}{\partial\eta}+3T_{2\mathrm{d}\,(\mathrm{i})}m_1\frac{\partial n_{2\mathrm{d}}^{(1)}}{\partial\xi}+3T_{2\mathrm{d}\,(\mathrm{i})}m_2\frac{\partial n_{2\mathrm{d}}^{(1)}}{\partial\eta}+ZM_{1\mathrm{d}\,(2\mathrm{d})}m_1\frac{\partial\phi^{(1)}}{\partial\xi}+ZM_{1\mathrm{d}\,(2\mathrm{d})}m_2\frac{\partial\phi^{(1)}}{\partial\eta}=0,\\
&n_{1\mathrm{d}}^{(1)}-Zn_{2\mathrm{d}\,(1\mathrm{d})}n_2^{(1)}+b_1\phi^{(1)}=0;
\end{aligned}
\tag{A1}
$$

$$
\begin{aligned}
&\bar{a}_1=\lambda_1^2\Big/\left(3T_{1\mathrm{d}(\mathrm{i})}\lambda_1^2-v_{\mathrm{ph}\,\xi}^2\right), && \bar{b}_1=\lambda_2^2\Big/\left(3T_{1\mathrm{d}(\mathrm{i})}\lambda_2^2-v_{\mathrm{ph}\,\eta}^2\right),\\
&\bar{a}_2=v_{\mathrm{ph}\,\xi}l_1\Big/\left(3T_{1\mathrm{d}(\mathrm{i})}\lambda_1^2-v_{\mathrm{ph}\,\xi}^2\right), && \bar{b}_2=v_{\mathrm{ph}\,\eta}l_2\Big/\left(3T_{1\mathrm{d}(\mathrm{i})}\lambda_2^2-v_{\mathrm{ph}\,\eta}^2\right),\\
&\bar{a}_3=v_{\mathrm{ph}\,\xi}m_1\Big/\left(3T_{1\mathrm{d}(\mathrm{i})}\lambda_1^2-v_{\mathrm{ph}\,\xi}^2\right), && \bar{b}_3=v_{\mathrm{ph}\,\eta}m_2\Big/\left(3T_{1\mathrm{d}(\mathrm{i})}\lambda_2^2-v_{\mathrm{ph}\,\eta}^2\right),\\
&c_1=ZM_{1\mathrm{d}(2\mathrm{d})}\lambda_1^2\Big/\left(3T_{2\mathrm{d}(\mathrm{i})}\lambda_1^2-v_{\mathrm{ph}\,\xi}^2\right), && \bar{c}_1=ZM_{1\mathrm{d}(2\mathrm{d})}\lambda_2^2\Big/\left(3T_{2\mathrm{d}(\mathrm{i})}\lambda_2^2-v_{\mathrm{ph}\,\eta}^2\right),\\
&c_2=ZM_{1\mathrm{d}\,(2\mathrm{d})}l_1v_{ph\xi}\Big/\left(3T_{2\mathrm{d}(\mathrm{i})}\lambda_1^2-v_{\mathrm{ph}\,\xi}^2\right), && \bar{c}_2=ZM_{1\mathrm{d}(2\mathrm{d})}l_2v_{ph\eta}\Big/\left(3T_{2\mathrm{d}\,(\mathrm{i})}\lambda_2^2-v_{\mathrm{ph}\,\eta}^2\right),\\
&c_3=ZM_{1\mathrm{d}\,(2\mathrm{d})}m_1v_{ph\xi}\Big/\left(3T_{2\mathrm{d}\,(\mathrm{i})}\lambda_2^2-v_{\mathrm{ph}\,\xi}^2\right),\\
&\bar{c}_3=ZM_{1\mathrm{d}\,(2\mathrm{d})}m_2v_{ph\eta}\Big/\left(3T_{2\mathrm{d}\,(\mathrm{i})}\lambda_2^2-v_{\mathrm{ph}\,\eta}^2\right);
\end{aligned}
\tag{A2}
$$

$$
\begin{aligned}
&C_{1\mathrm{N}}=\frac{1}{2}\left[\frac{v_{\mathrm{ph}\,\xi}X_1+l_1Y_1+m_1Z_1}{v_{\mathrm{ph}\,\xi}\bar{a}_1+l_1\bar{a}_2+m_1\bar{a}_3}-\frac{v_{\mathrm{ph}\,\xi}\bar{X}_1+l_1\bar{Y}_1+m_1\bar{Z}_1}{v_{\mathrm{ph}\,\xi}c_1+l_1c_2+m_1c_3}\right]+\frac{b_2}{b_1}\left[\frac{\lambda_1^2}{v_{\mathrm{ph}\,\xi}\bar{a}_1+l_1\bar{a}_2+m_1\bar{a}_3}+\frac{ZM_{1\mathrm{d}\,(2\mathrm{d})}\lambda_1^2}{v_{\mathrm{ph}\,\xi}c_1+l_1c_2+m_1c_3}\right],\\
&C_{1\mathrm{D}}=-\frac{\lambda_1^2}{2b_1}\left[\frac{\lambda_1^2}{v_{\mathrm{ph}\,\xi}\bar{a}_1+l_1\bar{a}_2+m_1\bar{a}_3}+\frac{ZM_{1\mathrm{d}\,(2\mathrm{d})}\lambda_1^2}{v_{\mathrm{ph}\,\xi}c_1+l_1c_2+m_1c_3}\right],\\
&C_{2\mathrm{N}}=\frac{1}{2}\left[\frac{v_{\mathrm{ph}\,\eta}X_4+l_2Y_4+m_2Z_4}{v_{\mathrm{ph}\,\eta}\bar{b}_1+l_2\bar{b}_2+m_1\bar{b}_3}-\frac{v_{\mathrm{ph}\,\eta}\bar{X}_4+l_2\bar{Y}_2+m_2\bar{Z}_4}{v_{\mathrm{ph}\,\eta}\bar{c}_1+l_2\bar{c}_2+m_2\bar{c}_3}\right]+\frac{b_2}{b_1}\left[\frac{\lambda_2^2}{v_{\mathrm{ph}\,\eta}\bar{b}_1+l_2\bar{b}_2+m_1\bar{b}_3}+\frac{ZM_{1\mathrm{d}\,(2\mathrm{d})}\lambda_2^2}{v_{\mathrm{ph}\,\eta}\bar{c}_1+l_2\bar{c}_2+m_2\bar{c}_3}\right],\\
&C_{2\mathrm{D}}=-\frac{\lambda_2^2}{2b_1}\left[\frac{\lambda_{21}^2}{v_{\mathrm{ph}\,\eta}\bar{b}_1+l_2\bar{b}_2+m_1\bar{b}_3}+\frac{ZM_{1\mathrm{d}\,(2\mathrm{d})}\lambda_2^2}{v_{\mathrm{ph}\,\eta}\bar{c}_1+l_2\bar{c}_2+m_2\bar{c}_3}\right],\\
&L=\frac{1}{2}\left[\frac{v_{\mathrm{ph}\,\xi}X_2+l_1Y_2+m_1Z_2}{v_{\mathrm{ph}\,\xi}\bar{a}_1+l_1\bar{a}_2+m_1\bar{a}_3}-\frac{v_{\mathrm{ph}\,\xi}\bar{X}_2+l_1\bar{Y}_2+m_1\bar{Z}_2}{v_{\mathrm{ph}\,\xi}c_1+l_1c_2+m_1c_3}\right]+\frac{b_2}{b_1}\left[\frac{\lambda_1^2}{v_{\mathrm{ph}\,\xi}\bar{a}_1+l_1\bar{a}_2+m_1\bar{a}_3}+\frac{ZM_{1\mathrm{d}\,(2\mathrm{d})}\lambda_1^2}{v_{\mathrm{ph}\,\xi}c_1+l_1c_2+m_1c_3}\right],\\
&M=\frac{1}{2}\left[\frac{v_{\mathrm{ph}\,\xi}\bar{X}_3-l_1\bar{Y}_3-m_1\bar{Z}_3}{v_{\mathrm{ph}\,\xi}c_1+l_1c_2+m_1c_3}+\frac{v_{\mathrm{ph}\,\xi}X_5-l_1Y_5-m_1Z_5}{v_{\mathrm{ph}\,\xi}\bar{a}_1+l_1\bar{a}_2+m_1\bar{a}_3}\right],\\
&L_1=\frac{1}{2}\left[\frac{v_{\mathrm{ph}\,\eta}X_3+l_2Y_3+m_2Z_3}{v_{\mathrm{ph}\,\eta}\bar{b}_1+l_2\bar{b}_2+m_1\bar{b}_3}-\frac{v_{\mathrm{ph}\,\eta}\bar{X}_5+l_2\bar{Y}_5+m_2\bar{Z}_5}{v_{\mathrm{ph}\,\eta}\bar{c}_1+l_2\bar{c}_2+m_2\bar{c}_3}\right]+\frac{b_2}{b_1}\left[\frac{\lambda_2^2}{v_{\mathrm{ph}\,\eta}\bar{b}_1+l_2\bar{b}_2+m_1\bar{b}_3}+\frac{ZM_{1\mathrm{d}\,(2\mathrm{d})}\lambda_2^2}{v_{\mathrm{ph}\,\eta}\bar{c}_1+l_2\bar{c}_2+m_2\bar{c}_3}\right],\\
&M_1=\frac{1}{2}\left[\frac{v_{\mathrm{ph}\,\eta}\bar{X}_6-l_2\bar{Y}_2+m_1\bar{Z}_6}{v_{\mathrm{ph}\,\eta}\bar{c}_1+l_2\bar{c}_2+m_2\bar{c}_3}+\frac{v_{\mathrm{ph}\,\eta}X_6-l_2Y_6-m_2Z_6}{v_{\mathrm{ph}\,\eta}\bar{b}_1+l_2\bar{b}_2+m_1\bar{b}_3}\right],\\
&X_1=2\bar{a}_1\bar{a}_2l_1+2\bar{a}_1\bar{a}_3m_1,\quad X_2=l_1\left(\bar{a}_1\bar{b}_2+\bar{a}_2\bar{b}_1\right)+m_1\left(\bar{a}_1\bar{b}_3+\bar{a}_3\bar{b}_1\right),\\
&X_3=l_2\left(\bar{a}_1\bar{b}_2+\bar{a}_2\bar{b}_1\right)+m_2\left(\bar{a}_1\bar{b}_3+\bar{a}_3\bar{b}_1\right),\quad X_4=2\bar{b}_1\bar{b}_2l_2+2\bar{b}_1\bar{b}_3m_2,\\
&X_5=v_{\mathrm{ph}\,\eta}\bar{a}_1-l_2\bar{a}_2-m_2\bar{a}_3,\quad X_6=v_{\mathrm{ph}\,\xi}\bar{b}_1-l_1\bar{b}_2-m_1\bar{b}_3,\\
&Y_1=l_1a_2^2+m_1\bar{a}_2\bar{a}_3+3T_{1\mathrm{d}(\mathrm{i})}l_1\bar{a}_1^2,\quad Y_2=l_1\bar{a}_3\bar{b}_2+m_1\bar{a}_2\bar{b}_3+3T_{1\mathrm{d}(\mathrm{i})}l_1\bar{a}_1\bar{b}_1,\\
&Y_3=l_2\bar{a}_2\bar{b}_2+m_2\bar{a}_3\bar{b}_2+3T_{1d(i)}l_2\bar{a}_1\bar{b}_1,\quad Y_4=l_2\bar{b}_1^2+m_2\bar{b}_3\bar{b}_2+3T_{1\mathrm{d}(\mathrm{i})}l_2\bar{b}_1^2,\\
&Y_5=3T_{1\mathrm{d}(\mathrm{i})}l_2\bar{a}_1-v_{\mathrm{ph}\,\eta}\bar{a}_2-l_2,\quad Y_6=3T_{1\mathrm{d}(\mathrm{i})}l_1\bar{b}_1-v_{\mathrm{ph}\,\xi}\bar{b}_2-l_1,\\
&Z_1=m_1a_3^2+l_1\bar{a}_2\bar{a}_3+3T_{1\mathrm{d}\,(\mathrm{i})}m_1\bar{a}_1^2,\quad Z_2=l_1\bar{a}_3\bar{b}_2+m_1\bar{a}_3\bar{b}_3+3T_{1\mathrm{d}\,(\mathrm{i})}m_1\bar{a}_1\bar{b}_1,\\
&Z_3=l_2\bar{a}_2\bar{b}_3+m_2\bar{a}_2\bar{b}_3+3T_{1\mathrm{d}\,(\mathrm{i})}m_2\bar{a}_1\bar{b}_1,\quad Z_4=m_2\bar{b}_3^2+l_2\bar{b}_2\bar{b}_3+3T_{1\mathrm{d}(\mathrm{i})}m_2\bar{b}_1^2,\\
&Z_5=3T_{1\mathrm{d}\,(\mathrm{i})}m_2\bar{a}_1+v_{\mathrm{ph}\,\eta}\bar{a}_3-m_2,\quad Z_6=3T_{1\mathrm{d}\,(\mathrm{i})}m_1\bar{b}_1-v_{\mathrm{ph}\,\xi}\bar{b}_3-m_1,
\end{aligned}
$$

$$\bar{X}_1 = 2\bar{a}_1\bar{a}_2 l_1 + 2\bar{a}_1\bar{a}_3 m_1, \quad \bar{X}_2 = l_1\left(\bar{a}_1\bar{b}_2 + \bar{a}_2\bar{b}_1\right) + m_1\left(\bar{a}_1\bar{b}_3 + \bar{a}_3\bar{b}_1\right),$$
$$\bar{X}_3 = v_{\mathrm{ph}\,\eta}\bar{a}_1 - l_2\bar{a}_2 - m_2\bar{a}_3, \quad \bar{X}_4 = 2\bar{b}_1\bar{b}_2 l_2 + 2\bar{b}_1\bar{b}_3 m_2,$$
$$\bar{X}_5 = l_2\left(\bar{a}_1\bar{b}_2 + \bar{a}_2\bar{b}_1\right) + m_2\left(\bar{a}_1\bar{b}_3 + \bar{a}_3\bar{b}_1\right), \quad \bar{X}_6 = v_{\mathrm{ph}\,\xi}\bar{b}_1 - l_1\bar{b}_2 - m_1\bar{b}_3,$$
$$\bar{Y}_1 = l_1 c_1^2 + m_1 c_2 c_{32} + 3T_{2\mathrm{d}\,(\mathrm{i})} l_1 c^2, \quad \bar{Y}_2 = l_1 c_3\bar{c}_2 + m_1 c_2\bar{c}_3 + 3T_{2\mathrm{d}\,(\mathrm{i})} l_1 c_1\bar{c}_1,$$
$$\bar{Y}_3 = 3T_{2\mathrm{d}\,(\mathrm{i})} l_2 c_1 - v_{\mathrm{ph}\,\eta} c_2 + ZM_{1\mathrm{d}\,(2\mathrm{d})} l_2, \quad \bar{Y}_4 = l_2\bar{c}_2^2 + m_2\bar{c}_2\bar{c}_2 + 3T_{2\mathrm{d}\,(\mathrm{i})} l_2\bar{c}_1^2,$$
$$\bar{Y}_5 = l_2 c_1\bar{c}_1 + m_2 c_2\bar{c}_2 + 3T_{2\mathrm{d}\,(\mathrm{i})} l_2 c_1\bar{c}_1, \quad \bar{Y}_6 = 3T_{2\mathrm{d}\,(\mathrm{i})} l_1 c_1 - v_{\mathrm{ph}\,\xi}\bar{c}_2 + ZM_{1\mathrm{d}\,(2\mathrm{d})} l_1,$$
$$\bar{Z}_1 = m_1 c_3^2 + l_1 c_2 c_3 + 3T_{2\mathrm{d}\,(\mathrm{i})} m_1 c_1^2, \quad \bar{Z}_2 = l_1 c_2\bar{c}_2 + m_1 c_3\bar{c}_3 + 3T_{2\mathrm{d}\,(\mathrm{i})} m_1 c_1\bar{c}_1,$$
$$\bar{Z}_3 = 3T_{2\mathrm{d}\,(\mathrm{i})} m_2 c_1 + v_{\mathrm{ph}\,\eta} c_3 - ZM_{1\mathrm{d}\,(2\mathrm{d})} m_2, \quad \bar{Z}_4 = m_2\bar{c}_3^2 + l_2\bar{c}_2\bar{c}_3 + 3T_{2\mathrm{d}\,(\mathrm{i})} m_2 c_1^2,$$
$$\bar{Z}_5 = l_2 c_2\bar{c}_3 + m_2 c_3\bar{c}_3 + 3T_{2\mathrm{d}\,(\mathrm{i})} m_2 c_1\bar{c}_1, \quad \bar{Z}_6 = v_{\mathrm{ph}\,\xi}\bar{c}_3 - 3T_{2\mathrm{d}(\mathrm{i})} m_1\bar{c}_1 + ZM_{1\mathrm{d}\,(2\mathrm{d})} m_1. \tag{A3}$$

References

[1] Shukla P K and Mamun A A 2002 *Introduction to Dusty Plasma Physics* (Bristol: IOP Publishing)
[2] Verheest F 2000 *Waves in Dusty Plasmas* (Dordrecht: Kluwer Academic)
[3] Shukla P K 2001 *Phys. Plasmas* **8** 1791
[4] Mendis D A and Rosenberg M 1994 *Ann. Rev. Astron. Astrophys.* **32** 419
[5] Saberiana E, Esfandyari-Kalejahib A and Afsari-Ghazib M 2017 *Plasma Phys. Rep.* **43** 83
[6] Dubinov A E 2009 *Plasma Phys. Rep.* **35** 991
[7] Gill T S, Bains A S and Bedi C 2010 *Phys. Plasmas* **17** 013701
[8] Tasnim I, Masud M M, Asaduzzaman M and Mamun A A 2013 *Chaos* **23** 013147
[9] Rao N N, Shukla P K and Yu M Y 1990 *Planet. Space Sci.* **38** 546
[10] Rao N N and Shukla P K 1994 *Space Sci.* **42** 221
[11] Melands? F and Shukla P K 1995 *Space Sci.* **43** 635
[12] Mamun A A, Shukla P K and Cairns R A 1996 *Phys. Plasmas* **3** 702
[13] Mamun A A, Shukla P K and Cairns R A 1996 *Phys. Plasmas* **3** 2610
[14] Mamun A A 1999 *Astrophys. Space Sci.* **268** 443
[15] Shukla P K and Mamun A A 2003 *New J. Phys.* **5** 17
[16] Mamun A A, Eliasson B and Shukla P K 2004 *Phys. Lett. A* **332** 412
[17] Chow V W, Mendis D A and Rosenberg M 1993 *J. Geophys. Res.* **98** 19065
[18] Chow V W, Mendis D A and Rosenberg M 1994 *IEEE Trans. Plasma Sci.* **22** 179
[19] Mamun A A and Shukla P K 2002 *Geophys. Res. Lett.* **29** 1870
[20] Fortov V E, Nefedov A P, Vaulina O S, Lipaev A M, Molotkov V I, Samaryan A A, Nikitskii V P, Ivanov A I, Savin S F, Kalmykov A V, Solovev A Y and Vinogradov P V 1998 *J. Exp. Theor. Phys.* **87** 1087
[21] Pierrard V and Lemaire J 1996 *J. Geophys. Res.: Space Phys.* **101** 7923
[22] Christon S P, Mitchell D G, Williams D J, Frank L A, Huang C Y and Eastman T E 1988 *J. Geophys. Res.: Space Phys.* **93** 2562
[23] Maksimovic M, Pierrard V and Lemaire J F 1997 *Astron. Astrophys.* **324** 725
[24] Pierrard V, Lamy H and Lemaire J 2004 *J. Geophys. Res.* **109** A02118
[25] Montgomery M D, Bame S J and Hundhause A J 1968 *J. Geophys. Res.* **73** 4999
[26] Feldman W C, Asbridge J R, Bame S J, Montgomery M D and Gary S P 1975 *J. Geophys. Res.* **80** 4181
[27] Pilipp W G, Miggenrieder H, Montgomery M D, Muhlhauser K H, Rosenbauer H and Schwenn R 1987 *J. Geophys. Res.* **92** 1075
[28] Maksimovic M, Pierrard V and Riley P 1997 *Geophys. Res. Lett.* **24** 1151
[29] Zouganelis I 2008 *J. Geophys. Res.* **113** A08111
[30] Magni S, Roman H E, Barni R, Riccardi C, Pierre Th and Guyomarc H D 2005 *Phys. Rev. E* **72** 026403
[31] Vasyliunas V M 1968 *J. Geophys. Res.* **73** 2839
[32] Hellberg M A, Mace R L, Armstrong R J and Karlstad G 2000 *J. Plasmas Phys.* **64** 433
[33] Hasegawa A, Mima K and Duong-Van M 1985 *Phys. Rev. Lett.* **54** 2608
[34] Baluku T K, Hellberg M A, Kourakis I and Saini N S 2010 *Phys. Plasmas* **17** 053702
[35] Lee M J 2010 *Curr. Appl. Phys.* **10** 1340
[36] Runmoni G, Roychoudhury R and Khan M 2011 *Indian J. Pure Appl. Phys.* **49** 173
[37] Alinejad H 2012 *Astrophys. Space Sci.* **339** 249
[38] Ghosh S, Sarkar S, Khan M and Gupta M R 2000 *Phys. Plasmas* **7** 3594
[39] Alinejad H and Mamun A A 2011 *Phys. Plasmas* **18** 112103
[40] Gourui M K, Chatterjee P and Wong C S 2013 *Astrophys. Space Sci.* **343** 639
[41] Su C H and Mirie R M 1980 *J. Fluid Mech.* **98** 509
[42] Jeffery A and Kawahawa T 1982 *Asymptotic Methods in Nonlinear Wave Theory* (London: Pitman)
[43] Huang G and Velarde M G 1996 *Phys. Rev. E* **53** 2988
[44] Xue J K 2004 *Phys. Rev. E* **69** 016403
[45] Li S C, Wu L H, Lin M M and Duan W S 2007 *Chin. Phys. Lett.* **24** 2312
[46] Han J N, Du S L and Duan W S 2008 *Phys. Plasmas* **15** 112104
[47] Chopra K N 2014 *Chin. J. Phys.* **52**
[48] Boruah A, Sharma S K, Bailug H and Nakamura Y 2015 *Phys. Plasmas* **22** 093706
[49] Das S 2019 *J. Phys.: Conf. Series* **1290** 012025
[50] Zahed H, Sayyar M R, Petehe S J and Sobahanian S 2018 *Int. J. Opt. Photon.* **12**
[51] Ferdousi M, Sultana S and Mamun A A 2015 *Phys. Plasmas* **22** 032117
[52] Paul S, Denra R and Sarkar S 2019 *AIP Conf. Proc.* **2072** 020014
[53] Chowdhury N A, Mannan A and Mamun A A 2017 *Phys. Plasmas* **24** 113701
[54] El-Shamy E F, Tribeche M and El-Taibany W F 2014 *Cent. Eur. J. Phys.* **12** 805
[55] Alam M S, Hafez M G, Talukder M R and Hossain A M 2018 *Phys. Plasmas* **25** 072904
[56] Chatterjee P and Ghosh U N 2011 *Euro. Phys. J. D* **64** 413